

Theo yêu cầu của khách hàng, trong một năm qua, chúng tôi đã dịch qua 16 môn học, 34 cuốn sách, 43 bài báo, 5 sổ tay (chưa tính các tài liệu từ năm 2010 trở về trước) Xem ở đây

**DỊCH VỤ
DỊCH
TIẾNG
ANH
CHUYÊN
NGÀNH
NHANH
NHẤT VÀ
CHÍNH
XÁC
NHẤT**

Chỉ sau một lần liên lạc, việc dịch được tiến hành

Giá cả: có thể giảm đến 10 nghìn/1 trang

Chất lượng: Tao dựng niềm tin cho khách hàng bằng công nghệ 1. Bạn thấy được toàn bộ bản dịch; 2. Bạn đánh giá chất lượng. 3. Bạn quyết định thanh toán.

Tài liệu này được dịch sang tiếng việt bởi:

www.mientayvn.com

Từ bản gốc:

<https://drive.google.com/folderview?id=0B4rAPqlxIMRDNkFJeUpfVUtLbk0&usp=sharing>

Liên hệ dịch tài liệu :

thanhlam1910_2006@yahoo.com hoặc frbwrthes@gmail.com hoặc số 0168 8557 403 (gặp Lâm)

Tìm hiểu về dịch vụ: http://www.mientayvn.com/dich_tiang_anh_chuyen_nganh.html

We propose a model of a nonlinear double-well potential NDWP, alias a double-well pseudopotential, with the objective to study an alternative implementation of the spontaneous symmetry breaking SSB in Bose-Einstein condensates BECs and optical media, under the action of a potential with two symmetric minima. In the limit case when the NDWP structure is induced by the local nonlinearity coefficient

Chúng tôi đề xuất mô hình NDWP giống thế kép phi tuyến, hay còn gọi là giả thế giống kép nhằm tìm kiếm một phương pháp khác để thực thi phá vỡ đối xứng tự phát SSB trong trạng thái ngưng tụ Bose-Einstein BEC và môi trường quang học, dưới tác động của thế có hai cực tiểu đối xứng. Trong trường hợp giới hạn khi cấu trúc NDWP được hình thành dưới tác động của hệ số phi tuyến cục bộ được biểu diễn qua tập hợp hai hàm delta,

represented by a set of two delta functions, a fully analytical solution is obtained for symmetric, antisymmetric, and asymmetric states. In this solvable model, the SSB bifurcation has a fully subcritical character. Numerical analysis, based on both direct simulations and computation of stability eigenvalues, demonstrates that, while the symmetric states are stable up to the SSB bifurcation point, both symmetric and emerging asymmetric states, as well as all antisymmetric ones, are unstable in the model with the delta functions. In the general model with a finite width of the nonlinear-potential wells, the asymmetric states quickly become stable, simultaneously with the switch of the SSB bifurcation from the subcritical to supercritical type. Antisymmetric solutions may also get stabilized in the NDWP structure of the general type, which gives rise to a bistability between them and asymmetric states. The symmetric states require a finite norm for their existence, an explanation to which is given. A full diagram for the existence and stability of the trapped states in the model is produced. Experimental observation of the predicted effects should be possible in BEC formed by several hundred atoms.

Introduce **10 h 46 phút**

The one-dimensional 1D Schrödinger equation including a symmetric potential structure produces single-particle wave functions of a definite parity, even or odd, with the ground state always corresponding to an even function without zeros. However, a spatially symmetric Hamiltonian of an interacting many-particle system can give rise to asymmetric states, which may be

chúng ta sẽ thu được một nghiệm hoàn toàn giải tích đối với các trạng thái đối xứng, phản đối xứng và bất đối xứng. Trong mô hình có thể giải được này, điểm rẽ nhánh SSB có đặc trưng hoàn toàn chưa tới hạn. Phân tích số dựa trên cả mô phỏng trực tiếp và tính toán các trị riêng ổn định cho thấy, trong khi các trạng thái đối xứng ổn định đến điểm rẽ nhánh SSB, trạng thái đối xứng và không đối xứng mới nổi lên cũng như tất cả các trạng thái phản đối xứng không ổn định trong mô hình có các hàm delta. Trong mô hình tổng quát với độ rộng giếng thế phi tuyến hữu hạn, các trạng thái bất đối xứng nhanh chóng trở nên ổn định, đồng thời chuyển các điểm rẽ nhánh SSB từ loại dưới tới hạn sang siêu tới hạn. Các nghiệm phản đối xứng cũng có thể ổn định trong cấu trúc NDWP loại tổng quát, làm nảy sinh hiệu ứng lưỡng ổn giữa chúng và các trạng thái phản đối xứng. Các trạng thái đối xứng cần chuẩn hữu hạn cho sự tồn tại của chúng và chúng ta sẽ giải thích vấn đề này. Chúng ta cũng sẽ xây dựng giản đồ đầy đủ về sự tồn tại và tính ổn định của các trạng thái bẫy trong mô hình. Quan sát thực nghiệm các hiệu ứng dự đoán là khả thi trong BEC được hình thành bởi vài trăm nguyên tử.

considered as a spontaneous-symmetry-breaking SSB effect. At the classical level, the SSB occurs in optics, as a result of the interplay between the nonlinearity and waveguiding structures, when the strong nonlinearity partly suppresses the linear coupling between parallel guiding cores. In particular, it was shown that a stable trapped mode may be asymmetric in a channel waveguide embedded in the self-focusing Kerr medium 1. The onset of a sharp symmetry-breaking instability in a double-hump two-component spatial optical soliton was demonstrated experimentally in a planar nonlinear waveguide 2. A natural setting in which SSB phenomena may arise in the context of nonlinear optics and Bose-Einstein condensation BEC is provided by double-well potentials DWPs. In the experiment, an effective optical DWP was created by a specially designed illumination pattern applied, in the ordinary polarization, to a photorefractive crystal the SSB was observed in a beam with extraordinary polarization, shone through this structure 3. It was also proposed to realize similar effective potentials in coupled nonlinear microcavities 4, and in a structured core of an optical fiber 5. A specific variety of the optical SSB was studied in a model of two parallel-coupled antiwaveguides (ống dẫn sóng có độ chênh lệch chiết suất giữa lõi và vỏ âm) with the self-focusing nonlinearity, which corresponds to an effective double barrier potential, rather than DWP 6. Well-known dual-core optical fibers 7, which may serve as a basis for the power-controlled all-optical switching, if the Kerr nonlinearity is taken into regard 8, may also be considered as DWP structures, with

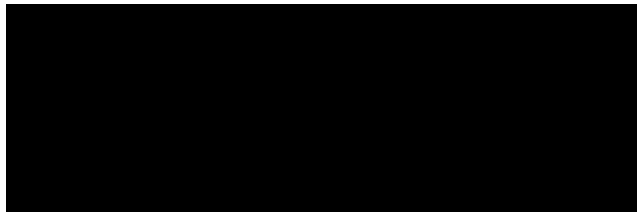
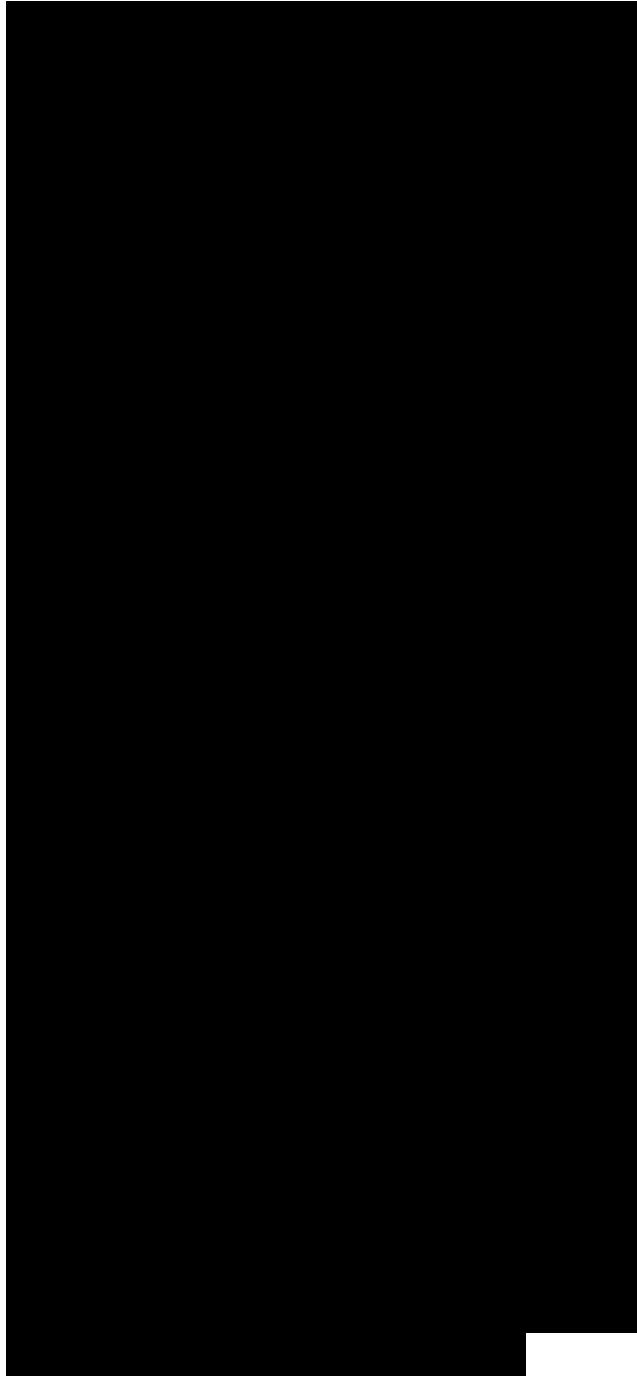
the difference that the tunneling between two potential wells is replaced by the linear coupling between the cores. In addition to the SSB of continuous-wave states 9, the formation of asymmetric solitons in dual-core fibers was studied in detail theoretically 10. Similar analysis of the SSB for soliton modes was performed in models of dual-core fiber Bragg gratings with the Kerr nonlinearity 11, and coupled waveguides with the quadratic 12 and cubic-quintic 13 nonlinear terms, including a system of linearly coupled complex Ginzburg-Landau equations of the cubic-quintic type 14. In Refs. 15–17, the analysis of the SSB was extended to three-core linearly coupled triangular configurations—for optical fibers, Bragg gratings, and complex Ginzburg-Landau equations, respectively. The concept of SSB also plays an important role in understanding experimental phenomena in BEC, because, if interactions between atoms are strong enough, the ground state of the condensate may not follow the symmetry of the trapping potential 18. In particular, manifestations of SSB were observed in a **quenched (bị dập tắt, làm lạnh)** ferromagnetic state of a spinor three-component condensate 19. In the single-component BEC, a natural setting for the realization of SSB may again be provided by DWP configurations. An effectively one-dimensional DWP structure was realized experimentally in Ref. 20. Loading a condensate of 87Rb atoms with the repulsive interaction between them into this structure made it possible to observe Josephson oscillations for a small number of atoms, and the macroscopic quantum self-trapping featuring an imbalance between populations of the two wells, for a larger

number. Parallel to the experimental work, numerous theoretical studies of matter-wave DWP settings have been performed for the cases of both repulsion and attraction between atoms. These studies addressed problems such as finite-mode reductions ²¹ including two-component mixtures ²², obtaining analytical results for specific shapes of the potential ²³, quantum effects ²⁴, and some others. Recently investigated tunneling between vortex and antivortex states in BEC trapped in a two-dimensional 2D anisotropic potential ²⁵ belongs to this category too. Theoretical analysis was also performed for 2D and 3D extensions of the DWP settings in BEC, which add one or two extra dimensions to the model, either without an additional potential, or with a periodic optical-lattice OL potential acting in these directions. These settings may be approximated, similar to the above-mentioned standard model of dual-core optical fibers, by a system of linearly coupled 1D ²⁶ or 2D ²⁷ equations. In a more accurate form, nearly 1D solitons can be found as solutions to the full 2D equation that includes the DWP the potential depends on the transverse coordinate x , allowing solitons to self-trap in the free longitudinal direction y ²⁸. The latter model is relevant to the case of the self-attractive nonlinearity. In the case of self-repulsion, dual-core gap solitons have been predicted in the setting with the OL potential applied along direction y ²⁹. Note that, in any setting, gap solitons cannot realize the ground state of the respective system, but, nevertheless, they represent stable configurations that have been created in the experiment using the condensate of ^{87}Rb atoms with the

repulsion between them 30.

~~A general principle, upheld by the analysis in various settings in nonlinear optics and BEC alike, is that the SSB occurs through bifurcations of symmetric or antisymmetric states, in the models with the self-attraction and self-repulsion, respectively. As mentioned above, models of the DWP or double-core type, combining cubic attractive and quintic repulsive nonlinearities, were studied too 13,14,31,32. In the latter case, the competition between the self-focusing and self-defocusing against the backdrop of the DWP structure gives rise to specific SSB bifurcation diagrams, in the form of nonconvex closed loops 13,32, as well as to specific dynamical switching regimes 31. Also predicted were manifestations of the SSB in a two-component BEC mixture trapped in the DWP structure 22, for both cases of the self-attraction and self-repulsion. All the extensive work on the SSB outlined above was performed in settings based on usual linear potentials of the double-well type. The objective of the present work is to propose another physical framework, in which the SSB can be predicted in an effective nonlinear double-well potential NDWP, induced through a spatial modulation of the local nonlinearity coefficient. Following the terminology commonly adopted in the solid-state theory 33, this nonlinear ingredient of the physical model may also be called a pseudopotential.~~

In BEC settings, a pseudopotential structure may be readily induced through spatial modulation of the local value of the s-wave scattering length, a_s , which determines the effective BEC



nonlinearity. The modulation can be implemented, through the Feshbach resonance, by means of a spatially inhomogeneous dc magnetic field 34, or by a resonant optical field, as predicted in Ref. 35 and demonstrated experimentally in Ref. 36. It was also proposed to control the Feshbach resonance by dint of dc electric field 37, which can be easily made inhomogeneous too. The attractive and repulsive interactions between atoms correspond to a_{s0} and a_{s0} , respectively; both signs, as well as sign-changing patterns, can be used to engineer effective nonlinear potentials. So designed pseudopotential lattices have attracted much interest in studies of BEC. In the 1D geometry, solitons, extended wave patterns, and various dynamical states supported by such structures were studied theoretically 38,39 a random nonlinear lattice 40 and pseudopotentials generated by a spatially monotonous ramp of the local scattering length 41 were explored too. Recently, similar states were also considered in nonlinear optics, assuming a periodic modulation of the local Kerr coefficient 42. Some but much fewer results were obtained too for 2D settings 43. However, to the best of our knowledge, SSB phenomena in nonlinear pseudopotentials have not been studied yet. In this work, we focus on such effects in NDWP settings, which can be engineered by means of techniques mentioned above, using attractive interactions between atoms in BEC, or the self-focusing nonlinearity in optics, as briefly described below. In Sec. II, we formulate the model and give estimates of characteristic values of related physical parameters. Section III reports full analytical solutions

corresponding to symmetric, antisymmetric, and asymmetric states trapped by the NDWP, in the limit case when the modulation of the local nonlinearity coefficient is represented by a set of two Dirac delta functions. The relevance of the latter model is stressed, in particular, by the recently introduced BEC model with a periodic nonlinear potential of the Kronig-Penney type, whose simplest version reduces to a periodic array of delta functions. SSB effects were not studied in Ref. 39. In Sec. IV, we present numerical results for the general model, in which the delta functions are replaced by a pair of Gaussians of a finite width. In that case, the trapped states are found in a numerical form, and their stability is studied by means of direct simulations of slightly perturbed stationary states and also, independently, through the computation of respective stability eigenvalues for small perturbations. The result is that asymmetric states, which are unstable in the delta-function limit, can be readily stabilized in the general model. In addition, antisymmetric states may be stabilized also, in two disjoint regions of the parameter space, giving rise to a bistability involving antisymmetric and asymmetric states. A condition for the existence of symmetric states is that their norm must exceed a certain threshold value, in terms of their norm, an explanation to which is given. The existence and stability of all states, including a line of the SSB bifurcation, are summarized in a single diagram, which is presented in Sec. IV also. Results reported in this paper and perspectives for further work are summarized in Sec. V.

Model

The underlying 3D Gross-Pitaevskii equation for the mean-field wave function.

For physical parameters relevant to experiments with the condensate of ^7Li atoms 45 , i.e., a_2 m, $A00.5$ nm, and 20 m, characteristic values of the number of atoms in various patterns reported below see, in particular, Figs. $3d$ and 9 fall into the range of N between 200 and 1000 , which is quite sufficient for experimental manipulations and observation of the patterns. In the same range of physical parameters, $t=1$ in Eq. 5 is estimated as being tantamount to 10 ms, hence typical time scales for the instability development or intrinsic oscillations of breathers induced by the instabilities, which are reported below, are expected to be in the range of $0.1-1$ s, which is realistic to the currently available experimental techniques 45 .

In terms of optical settings, a set of two narrow of width 1 μm parallel stripes with strong local nonlinearity can be built, in a planar waveguide, by means of known nanotechnological methods. In that case, the power of the laser beam necessary for the self-trapping of transverse nonlinear patterns in the waveguide made of silica may be 500 kW 46 , while using AlGaAs, one may reduce the necessary power to the level of 1 kW 47 . In these settings, the characteristic evolution length of the spatial beam can be made shorter than 1 mm. Obviously, transitions between states of different types reported in this paper may be relevant to the design of power-controlled optical-switching schemes. On the other hand, the description of the planar waveguide with the pair of embedded

stripes may require a model more general than the one studied here, as it will plausibly combine the transverse modulation of the local nonlinearity with a similar linear potential which is briefly described at the end of the next section, as the material difference between the stripes and host medium ought to affect the linear index of refraction also.

The analytical solution given by Eqs. 13, 14, and 24 make it possible to plot the bifurcation diagrams in the planes of a and N , which are represented by curves pertaining to $a=0$ in Figs. 3a–3c. To generate the diagrams, partial norms N in expression 25 for the asymmetric solutions were computed numerically; analytical expressions for them are available, but they are very messy, cf. Eq. 21 for the symmetric and antisymmetric states. A salient peculiarity of the SSB bifurcation for $a=0$, evident in Fig. 3c, is its subcritical character, which means that the branches of asymmetric solutions emerge at the bifurcation point as unstable ones, and go in the backward direction. A subcritical bifurcation also occurs in the above-mentioned model of the dual-core nonlinear fibers 10, but in that case the asymmetric branches quickly turn in the forward direction, getting stabilized at the turning point. A remarkable feature of the present model with $a=0$ is that this does not happen, i.e., the bifurcation in this model may be called a “fully backward” one: the branches of the asymmetric solutions keep going backward up to the limit of $a=1$, which corresponds to the asymmetric solutions with $a=1$ and $N=1$, as shown in the following subsection. Indeed, $a=1$ follows from the fact that the amplitude

appertaining to the lower sign between the radicals in Eq. 24 vanishes in the limit of $\rightarrow -$.

.....
In accordance with general properties of the subcriticalSSB bifurcation [10], the symmetric solution is expected to be stable below the bifurcation point at $N=N_{bif}$, see Eq.23, and unstable above it. The asymmetric branches emerging at $N=N_{bif}$ are unstable as long as they go backward. In the present case $a=0$, this means they are always unstable, as the respective branches in Figs. 3b and 3c never turn forward. All these expectations are completely borne out by the stability analysis performed by means of both direct simulations and computation of stability eigenvalues, at finite but small values of a . Technical details of the procedure are described in the next section. In particular, at $N=N_{bif}$ the unstable symmetric state spontaneously transforms into a strongly asymmetric breather (một sóng phi tuyến có năng lượng tập trung theo kiểu cục bộ hoặc dao động) which features irregular oscillations, but remains robust as a whole quite similar to an example displayed below in Fig. 6 for $a=0.7$. On the other hand, unstable asymmetric states transform themselves into breathers which maintain the original asymmetry of the unstable state, as shown in Fig. 4. Lastly, all antisymmetric states in the model with delta functions are unstable too. Their instability is similar to that shown below in Fig. 7b for $a=1$, transforming them into strongly asymmetric breathers. As shown in the next section, both asymmetric and antisymmetric states may be stabilized in the general model, with finite a .

The existence of the asymmetric states, i.e., the presence of the SSB effect in the present model, can be easily explained by the consideration of the above-mentioned limit of $\rightarrow -$. Indeed, in this limit, the spatial scale of the solution, which is $\sim 1/2$ according to Eq. 13, is much smaller than the separation between the two delta functions, $2L$. Therefore, the full solution effectively splits into a superposition of those independently supported by each delta function in isolation. Further, it is obvious that, for given large L , Eq. 12 with an individual delta function gives rise to two solutions: a trivial one.

where or note that the norm of solution 26 is $N=1$, for any L . The corresponding symmetric and antisymmetric states are built, respectively, as superpositions of solutions $+$ or, equivalently, $-$ centered at $x=-1$ and $x=+1$, or centered at $x=-1$ and $+$ centered at $x=+1$. Asymmetric solutions are represented, in the same limit, by a superposition of solution centered at $x=-1$ and zero solution around $x=+1$, or vice versa. Of course, finding a bifurcation point requires one to perform the analysis of the model at finite L , as done in the analytical form above for the case of the delta functions, and will be done in a numerical form below for the general case of finite a in Eq. 6. It is relevant to compare the above exact results with those which can be easily obtained in the linear counterpart of the model, i.e., the one with the DWP based on the set of two delta functions; as mentioned above, such a linear potential may be a plausible ingredient of a more general model, relevant to the description of NDWP settings in optics. The stationary version of the linear equation reduces to.

B. Results

The first significant change against the results reported above for the model with the delta functions $a=0$, which happens with the increase of a , is quick stabilization of asymmetric states with larger values of the norm, while ones with smaller N remain unstable, originally. At $a=0.2$, the symmetric states are stable for all values of N at which they exist. Another notable feature of the bifurcation diagrams at finite a , demonstrated by Figs. 3b and 3d, is that the norm at which the SSB bifurcation takes place, N_{bif} , first decreases with the growth of a from small values up to $a=0.8$, and then increases with the further growth of a .

Close to their stabilization threshold in particular, at $a=0.2$, asymmetric states with a smaller norm, which are still unstable, demonstrate a scenario of the instability development different from what was shown by their counterpart in Fig. 4 in the case of very small a . Namely, slow regular oscillations, observed in Fig. 5 in this case, imply a dynamical resymmetrization of the unstable asymmetric state. Indeed, densities x_2 , taken at points $x=1$, perform identical periodic oscillations, with a phase shift of π between them, as shown in Fig. 5b.

The stabilization of the asymmetric states at small finite values of a is explained by the change in the character of the SSB bifurcation: at $a=0$, there appear turning points on branches of asymmetric solutions in the bifurcation diagram, cf. Fig. 3c. Past the turning point, the branch

goes forward as a stable one. In fact, Fig. 3c demonstrates a quick transformation, with the increase of a , of the subcritical bifurcation into a supercritical one. When the bifurcation is supercritical, branches of the asymmetric solutions emerge as stable ones at the bifurcation point, and immediately go forward. We do not display the quick transition from the sub-to-supercritical bifurcation in full detail, as it actually happens at very small a , in the range of $a \approx 0.1$. The physical estimates given in Sec. II suggest that so small values of the scaled width of the nonlinear-potential wells correspond to physical widths ~ 1 m. It seems doubtful that the Feshbach-resonance technique would allow one to create a strong local inhomogeneity of the scattering length on such a small scale nevertheless, the exact analytical solutions obtained for $a=0$, which provide clear clues for the understanding of the general model, are definitely relevant. An additional problem impeding the full analysis of the case of very small a is that, in this case, the accumulation of systematic numerical results requires very heavy simulations, as the step size of the spatial grid must be made much smaller than a . Above the bifurcation point, symmetric states found at finite a demonstrate the familiar SSB instability, spontaneously transforming themselves into slightly nonstationary robust modes breathers, quite close in their shape to respective stable asymmetric solitons. A typical example of this transformation is displayed in Fig. 6. As concerns antisymmetric solutions, both stable and unstable ones have been found at finite a , as illustrated by Figs. 7 and 8. Figure 7b shows that the density profile of unstable antisymmetric states evolves from the double-peak pattern into

an asymmetric single-peak one, which features persistent intrinsic oscillations. This outcome of the instability development complies with the fact that the instability of the antisymmetric states is oscillatory, being accounted for by a quartet of eigenvalues, as seen in Fig. 8b. In other words, the transition from stable to unstable antisymmetric states may be considered as the Hamiltonian Hopf bifurcation [48]. Figure 9 displays a combined diagram in the plane of the norm of the solution and width of the nonlinear potential wells, N and a , which summarizes the existence and stability results for the states of all three types—symmetric, asymmetric, and antisymmetric ones. The dashed-dotted line in the figure designates the symmetry-breaking bifurcation. Solely symmetric states exist below this line; they are stable in that region, and stable asymmetric states exist above the line, where the symmetric ones are unstable. Solid curves in Fig. 9 depict stability borders of antisymmetric solutions. For the reasons explained above, the region of very small values of a , where the “quick” stabilization of asymmetric states takes place, is not included. However, the region of the existence of the analytical symmetric and antisymmetric solutions in the model with delta functions $a=0$, and the respective bifurcation point, as given by Eq. 23, are shown by the bold vertical segment and square-marked dot on the axis of $a=0$. Recall that the exact asymmetric solutions are unstable above the bifurcation point in the model with $a=0$.

~~Because the modulation profile ϕ does not feature the double-well structure for~~

~~a_2 see Fig. 1, the SSB bifurcation tends to disappear as a approaches 2.~~ Actual results are included in Fig. 9 for $a=1.35$, as the convergence of the numerical scheme becomes poor for values of a still closer to 2. The chain of circles in Fig. 9 designates the threshold minimum norm N_{\min} , necessary for the existence of symmetric states in the model. As mentioned above, in the case of $a=0$ the exact threshold is $N_{\min}(a=0)=\sqrt{2}$, and it is observed in Fig. 9 that the threshold remains in the ballpark of this value at finite a , which can be easily explained. Indeed, the minimum of N is attained at $\lambda \rightarrow -0$, in which limit the spatial scale of the wave function, λ^{-1} , is much larger than the size of the NDWP structure, $2L$. Thus, from the viewpoint of this weakly localized wave function, modulation pattern 6 looks like 2x. In the corresponding approximation, the wave function takes the form of expression 26 divided by 2, and the respective norm is, indeed, $\sqrt{2}$. For $N \geq N_{\min}$, the condensate confined to the trap of large length L i.e., in the thermodynamic limit will tend to form a quasiuniform nearly linear state, with $x = \sqrt{2}L$. As follows from Eqs. 8 and 6, the energy of the small-amplitude uniform state is $H_0 - N^2 L^4$. ³³In fact, this state realizes a minimum of the energy cf. Fig. 10, i.e., the system's ground state. Nevertheless, a well-known fact is that dynamically stable localized states different from the ground state, such as the above-mentioned gap solitons in the repulsive condensate ³⁰, or their broader counterparts in the form of the so-called gap waves ⁴⁹, can be created in the experiment.

Another notable feature observed in Fig. 9 is the bistability, i.e., the coexistence of

stable asymmetric and antisymmetric states above the stability border of the latter state. In fact, the bistability always takes place when antisymmetric states are stable. It is interesting too that the stability area for the antisymmetric states consists of two separate regions. Finally, it is relevant to mention that, as well as in the analytically solvable model with the delta functions $a \rightarrow 0$, the antisymmetric states never undergo a bifurcation at finite a . We stress that the stability borders displayed in Fig. 9 were identified by means of direct simulations and the computation of stability eigenvalues, both methods yielding identical results. In particular, the sets of eigenvalues displayed in Fig. 8 clearly confirm the presence of two disjoint stability areas for antisymmetric states.

In the case of the bistability involving the asymmetric and antisymmetric states, it is interesting to compare their energy values of the Hamiltonian. To this end, Fig. 10 displays a typical example of the dependence of H on norm N . The situation observed in this figure is also true in the general case: stable antisymmetric states realize smaller values of H than the asymmetric counterparts coexisting with them. However, as argued above, dynamically stable states can be created in the experiment even if their energy is higher than in some competing states. In particular, Fig. 6 demonstrates that an unstable symmetric state definitely self-traps into an asymmetric robust breather which is close to a stable stationary solution, despite the fact that a stable antisymmetric state exists at the same values of $N=10$ and $a=0.7$, as seen from Fig. 9. Note that all curves in Fig. 10 start from finite threshold values of N corresponding, as said above, to the

minimum norm N_{\min} necessary for the existence of the respective states. In particular, for the branch of symmetric solutions, N_{\min} is close to $\bar{1}2$, as argued above cf. the existence border in the bottom of Fig. 9, while the asymmetric branch originates at the bifurcation point in agreement with the location of the respective dashed-dotted line in Fig. 9, at which the symmetric solution loses its stability. The branch of antisymmetric solutions features a fold in Fig. 10 in the region where these solutions are unstable, which is similar to the above-mentioned fact that dependence N_{in} Eq. 21 for the unstable exact antisymmetric states has a minimum, $N_{\text{antisymmin}} = 1.84$ at -0.58 . If replotted in terms of H and N , Eq. 21 features a similar fold, at $N = N_{\text{antisymmin}}$.

V. CONCLUSION

In this work, we have introduced a model of the NDWP, alias a double-well pseudopotential, which can be created in BEC, by means of the spatially inhomogeneous Feshbach resonance, and also in nonlinear optics. The model provides for a previously unexplored setting in which effects of the SSB can be studied.

In the limit when each potential well is induced by the δ -function, full analytical solutions were obtained for symmetric, antisymmetric, and asymmetric states. The symmetric states are stable in that case up to the symmetry-breaking bifurcation point, but beyond the bifurcation both symmetric and emergent asymmetric states are unstable. In particular, the asymmetric configurations transform themselves into

breathers. The instability of all the stationary asymmetric states in the model with the delta functions is explained by the fact that the respective SSB bifurcation is of a “fully backward” type, with branches of the asymmetric solutions never turning forward. All antisymmetric states are unstable too, in this limit form of the model. The increase of the width of the potential wells readily stabilizes the asymmetric states, which concurs with the change of the character of the SSB bifurcation from sub- to supercritical. Close to the stabilization border, unstable asymmetric states develop slow intrinsic oscillations, featuring effective dynamical resymmetrization.

Antisymmetric states may also be stable in the NDWP structure with a finite width of the wells, which implies the bistability between asymmetric and antisymmetric states. The symmetric states exist above a finite threshold, in terms of the number of atoms in the condensate, and they develop the usual SSB instability above the bifurcation point. A simple explanation to the existence threshold was given, and an integrated diagram for the existence and stability of the trapped states of all three types has been produced.

The analysis presented in this work suggests new experiments in the matter-wave and nonlinear-optical settings. The analysis can also be developed in other directions. In particular, it may be interesting to study a two-dimensional nonlinear-DWP configuration. In the 2D space, a triangular configuration with three nonlinear pseudo-potential wells may be considered too.

--	--